

Electron acceleration during magnetic islands coalescence and division process in a guide field reconnection

Shengxing Han(韩圣星), Huanyu Wang(王焕宇), and Xinliang Gao(高新亮)
Citation: Chin. Phys. B, 2022, 31 (**2**): 025202. DOI: 10.1088/1674-1056/ac21c0
Journal homepage: http://cpb.iphy.ac.cn; http://iopscience.iop.org/cpb

What follows is a list of articles you may be interested in

Spontaneous growth of the reconnection electric field during magnetic reconnection with a guide field: A theoretical model and particle-in-cell simulations

Kai Huang(黄楷), Quan-Ming Lu(陆全明), Rong-Sheng Wang(王荣生), Shui Wang(王水)
Chin. Phys. B, 2020, 29 (**7**): 075202. DOI: 10.1088/1674-1056/ab8da0

Basic features of the multiscale interaction between tearing modes and slab ion-temperature-gradient modes

L Wei(魏来), Z X Wang(王正汹), J Q Li(李继全), Z Q Hu(胡朝清), Y Kishimoto(岸本泰明)
Chin. Phys. B, 2019, 28 (**12**): 125203. DOI: 10.1088/1674-1056/ab5437

Formation of electron depletion layer and parallel electric field in the separatrix region of anti-parallel magnetic reconnection

Zisheng Li(李子圣), Huanyu Wang(王焕宇), Xinliang Gao(高新亮)
Chin. Phys. B, 2019, 28 (**7**): 075203. DOI: 10.1088/1674-1056/28/7/075203

Numerical study of fast ion behavior in the presence of magnetic islands and toroidal field ripple in the EAST tokamak

Zhang Wei, Hu Li-Qun, Sun You-Wen, Ding Si-Ye, Zhang Zi-Jun, Liu Song-Lin
Chin. Phys. B, 2014, 23 (**10**): 105201. DOI: 10.1088/1674-1056/23/10/105201

Out-of-plane shear flow effects on fast magnetic reconnection in a two-dimensional hybrid simulation model

Wang Lin, Wang Xian-Qu, Wang Xiao-Gang, Liu Yue
Chin. Phys. B, 2014, 23 (**2**): 025203. DOI: 10.1088/1674-1056/23/2/025203

Electron acceleration during magnetic islands coalescence and division process in a guide field reconnection

Shengxing Han(韩圣星)[1,2], Huanyu Wang(王焕宇)[1,2,†], and Xinliang Gao(高新亮)[1,2]

[1] *CAS Key Laboratory of Geospace Environment, School of Earth and Space Sciences, University of Science and Technology of China, Hefei* 230026, *China*
[2] *CAS Center for Excellence in Comparative Planetology, Hefei* 230026, *China*

(Received 13 April 2021; revised manuscript received 1 August 2021; accepted manuscript online 27 August 2021)

The magnetic merging process related to pairwise magnetic islands coalescence is investigated by two-dimensional particle-in-cell simulations with a guide field. Owing to the force of attraction between parallel currents within the initial magnetic islands, the magnetic islands begin to approach each other and merge into one big island. We find that this newly formed island is unstable and can be divided into two small magnetic islands spontaneously. Lastly, these two small islands merge again. We follow the time evolution of this process, in which the contributions of three mechanisms of electron acceleration at different stages, including the Fermi, parallel electric field, and betatron mechanisms, are studied with the guide center theory.

Keywords: magnetic reconnection, magnetic islands, electron acceleration, particle-in-cell simulation

PACS: 52.35.Vd, 52.65.–y, 52.65.Rr, 94.20.wc **DOI:** 10.1088/1674-1056/ac21c0

1. Introduction

As a fundamental physical process in space plasma, magnetic reconnection has a close connection with rapid energy conversion, where magnetic field releases free energy suddenly and then accelerates and heats the plasma.[1–4] It is considered that energetic electrons are closely bound up with magnetic reconnection, which associated with explosive phenomena in laboratory and space plasma, like solar flares in the solar atmosphere,[5–7] substorms in the Earth's magnetosphere,[8–10] and disruptions in laboratory fusion experiments.[11,12] The electron acceleration mechanisms have been fruitfully studied during magnetic reconnection.[13–24] In the vicinity of the X line, electrons can be accelerated by the reconnection electric field,[13–16] by the Fermi mechanism in the contracting sites of magnetic islands,[17,18] by the betatron mechanism in the magnetic field pile-up region to the dipolarization front,[19–22] and by the acceleration of parallel electric fields in the separatrix region.[23–25] With the help of adiabatic theory (also called guide-center theory),[26] the contributions of Fermi, parallel electric fields and betatron mechanisms have been studied quantitatively. In 2D simulations, several studies found that the guide field controls contributions of the above-mentioned mechanisms playing a leading role in electron energy gain.[27–29] In weak guide field cases, the Fermi mechanism dominates electron acceleration.[30–32] When the value of the guide field increases, the Fermi mechanism plays less important part in electron acceleration. On the contrary, the parallel electric field acceleration is the dominate driver for electron energization with the guide field increasing sufficiently.[28–30] The adiabatic theory has also been used in the 3D magnetic reconnection in a guide field to study the temporal development of parallel electric field acceleration and Fermi acceleration.[33,34]

During multiple X line reconnection, the formation of magnetic islands between two X lines is considered to enhance not only the reconnection rate but also the efficiency of particle acceleration.[17,18,31,35–37] In magnetic reconnection, it has been observed that the coalescence of magnetic islands takes place in Earth's magnetotail,[38–40] at the magnetopause,[41] and along the current sheet in a coronal mass ejection.[42] Magnetic islands or plasmoid can also be observed in the near venusian magnetotail, as a evidence of magnetic reconnection.[43] In the simulation of this paper, the electron acceleration through the magnetic islands coalescence is investigated with a 2D particle-in-cell (PIC) simulation. The initial state of the simulation domain is the island-chain equilibrium with a guide field, in which two magnetic islands are placed. Owing to the force of attraction between parallel currents within the two initial magnetic islands, the magnetic islands begin to approach each other. After the coalescence of the two islands into one new island, this newly formed island split into two small magnetic islands spontaneously. Lastly, these two small islands merge again. We follow the time evolution of the spontaneous division of the magnetic island, which shows a more complex process than our expectancy of the story after the magnetic island coalescence. With the guide center theory, we study the contributions of three kinds of electron acceleration mechanisms at different stages, including the Fermi, parallel electric field, and betatron mechanisms.

There is the organization of this paper as follows. Our simulation model is delineated in Section 2. In Section 3, the

†Corresponding author. E-mail: iuwon@mail.ustc.edu.cn

© 2022 Chinese Physical Society and IOP Publishing Ltd

simulation results are given. Summary of results and their significance are discussed in Section 4 lastly.

2. Simulation model

This paper uses 2D PIC simulations to investigate the electron acceleration process throughout the coalescence of magnetic islands. In our PIC simulations, the Maxwell equation is solved through a full explicit algorithm to define and update the electromagnetic fields on the grids, where ions and electrons are advanced. The island-chain equilibrium is set to the initial configuration.[35] The magnetic field vector potential is given by

$$A_{0y}(x,z) = -LB_0 \ln[\cosh(z/L) + \varepsilon\cos(x/L)], \tag{1}$$

where L represents the half-thickness of the current sheet in z, and B_0 is the asymptotic value of the x component of the magnetic field. The parameter ε $(0 \le \varepsilon < 1)$ is important for determining the width of the initial island chain by

$$\frac{z}{L} = \cosh^{-1}(1+2\varepsilon). \tag{2}$$

We take $\varepsilon = 0.9$ in the simulation of this paper. The half-thickness of the current sheet $L = 0.8d_\mathrm{i}$. The simulation is initialized with pairwise magnetic islands of the infinite island chain. A periodic boundary condition is assumed in x, while the boundary condition in z is assumed to be reflective. The initial density distribution is

$$n(x,z) = n_\mathrm{b} + n_0 \frac{1-\varepsilon^2}{[\cosh(z/L)+\varepsilon\cos(x/L)]^2}, \tag{3}$$

where n_b gives the value of density of a uniform, nondrifting background plasma and $n_\mathrm{b}/n_0 = 0.2$. The initial electrons and ions satisfy Maxwell velocity distribution. In this simulation, the ion-to-electron mass ratio is $m_\mathrm{i}/m_\mathrm{e} = 100$, the light speed $c = 15v_\mathrm{A}$, where v_A is the Alfvén speed based on B_0 and n_0, and the temperature ratio is $T_\mathrm{i0}/T_\mathrm{e0} = 4$. This simulation is performed in a rectangular domain with the grid number $N_x \times N_z = 200 \times 300$ and the size $L_x \times L_z = 10d_\mathrm{i} \times 15d_\mathrm{i}$, where d_i is the ion inertia length. Therefore, the spatial resolution can be calculated to be $\Delta x = \Delta z = 0.05d_\mathrm{i}$. The ion gyrofrequency can be given by $\Omega_\mathrm{i} = eB_0/m_\mathrm{i}$ and the simulation time step is set to $\Omega_\mathrm{i}\Delta t = 0.001$. There are more than 10^6 particles per species for more accurate simulation results. The initial guide magnetic field is $B_{y0} = 0.5B_0$, and the initial electron $\beta_\mathrm{e} = 0.2$. In the vicinity of the reconnection site, constrained by the guide field, the local electron Larmor radius is $\sim 0.1d_\mathrm{i}$, which is smaller than the half thickness of the current sheet L. It is almost kept to be adiabatic for electron motions so that the guide-center approximation could be satisfied.

3. Simulation results

We firstly analyze the time evolution of these two magnetic islands. Figure 1 plots the electric field E_y from $\Omega_\mathrm{i}t = 20$ to 25. In the figure there are the magnetic field lines plotted as reference. The whole process can be clearly divided into three stages. Figures 1(a)–1(c) indicate the first stage where two magnetic islands approach and then are merge into a new island. In virtue of the force of attraction between initial parallel currents, the magnetic islands begin to approach each other in the beginning of the simulation.

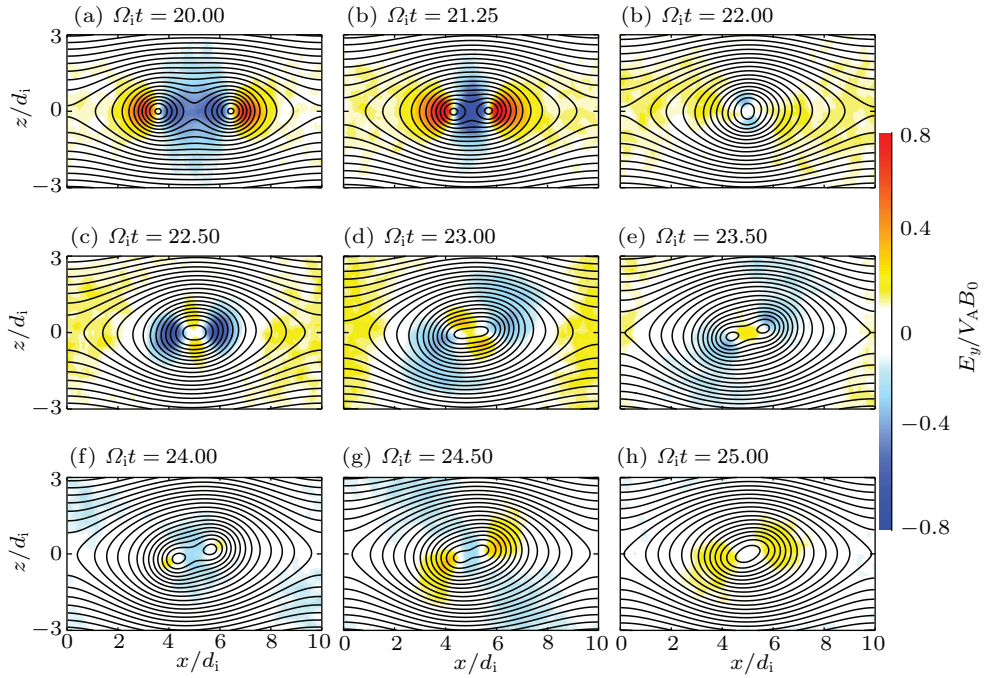


Fig. 1. The time evolution of electric field E_y and magnetic field lines from $\Omega_\mathrm{i}t = 20$ to 25.

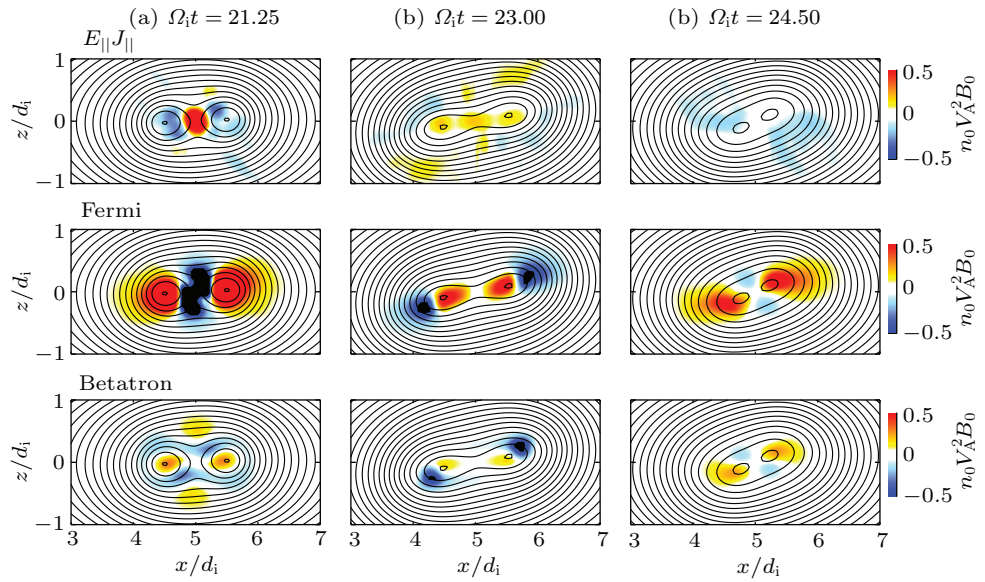


Fig. 2. The spatial distribution of contributions to electrons acceleration of the parallel electric field, Fermi, and betatron mechanisms at (a) $\Omega_i t = 21.25$, (b) 23, and (c) 24.5.

From $\Omega_i t = 20$ to 21.25, E_y increases in the vicinity of the reconnection site with a negative value, where two islands merge at the center of the simulation area ($x \sim 5d_i, z \sim 0d_i$). The coalescence of these two magnetic islands into one new island ends at about $\Omega_i t = 22$. Figures 1(d)–1(f) show the second stage. The magnetic island expands in the x direction from $\Omega_i t = 22.5$ to 23, which divide into two small magnetic islands at $\Omega_i t = 23.5$. In this stage, E_y increases in the vicinity of the reconnection site with a positive value, when these two newly formed islands gradually are drew apart. In the third stage, as indicated in Figs. 1(g) and 1(h), these two islands begin to approach each other and finally are merged into one island at $\Omega_i t = 25$. The process is similar to the first stage with the weaker strength of E_y, which is due to the decrease of the reconnection rate.

In Fig. 2, it shows the contributions of the three kinds of mechanisms at $\Omega_i t = 21.25$, 23 and 24.5, in which contributions are calculated based on the guide-center theory:[26,27]

$$\frac{\mathrm{d}U}{\mathrm{d}t} = E_{\|}J_{\|} + \frac{P_{\perp}}{B}\left(\frac{\partial B}{\partial t} + \boldsymbol{u}_{\mathrm{E}}\cdot\nabla B\right) + (p_{\|} + m_{\mathrm{e}}nu_{\|}^2)\boldsymbol{u}_{\mathrm{E}}\cdot\boldsymbol{\kappa}, \quad (4)$$

where U is the total electron kinetic energy, $\boldsymbol{u}_{\mathrm{E}}$ is the $\boldsymbol{E}\times\boldsymbol{B}$ drift velocity, $u_{\|}$ is the electron bulk velocity parallel to the ambient magnetic field, n is the electron density, and $p_{\|}$ and $p_{\perp}$ are the electron perpendicular and parallel pressures, respectively. In Eq. (4), the electron acceleration by the parallel electric field is represented by the first term on the right side. The betatron mechanism is represented by the second term, as a result of the conservation of the electron magnetic moment. The last term indicates the first-order Fermi mechanism, which drives electron acceleration in the parallel direction.

The first stage of the process is shown in Fig. 2(a), where two islands are merging at $\Omega_i t = 22.5$. Strong positive effect of parallel electric field acceleration can be found in the vicinity of the X line, which is due to the contribution of the reconnection electric field. Electrons can also be accelerated by the Fermi mechanism at the contracting sides of the magnetic islands, which is related to the "head-to-head collision" between the electron guide-center and the contracting side of the magnetic island.[26] However, in the vicinity of the X line, the Fermi mechanism is negative at the approaching sides of the magnetic islands, which is related to the head-to-tail collision, similar results with the previous works.[27–33] Note that the negative contribution of the betatron mechanism around the merging site, which due to the weakening of the local magnetic strength $B = \sqrt{B_x^2 + B_y^2 + B_z^2}$. The second stage is shown in Fig. 2(b) at $\Omega_i t = 30$, where the newly formed magnetic island expands in the x direction, and is divided into two small magnetic islands. Positive effect of parallel electric field acceleration can still be found in the vicinity of the X line, with the reconnection electric field getting weaker compared with the results shown in the first stage. As the two islands separates from each other, the Fermi mechanism shows positive in the vicinity of the X line and negative at two expanding ends of the islands. The betatron mechanism is locally strong at the expanding ends of these two magnetic islands, which cannot be neglected. Figure 2(c) shows the third stage where these two small magnetic islands are merging. The process is similar to the first stage, in which electron acceleration is dominant by the Fermi mechanism. The contribution from the parallel electric field is not obvious in this stage due to the decrease of the reconnection rate.

For the sake of evaluating different electron acceleration mechanisms, we plot the time evolution of the spatially integrated contribution of the three mechanisms to the electron acceleration: Fermi (red), parallel electric field (blue) and betatron (black) in Fig. 3(a). In the first stage, two magnetic

islands begin to approach each other due to the force of attraction between initial parallel currents. The Fermi contribution rises quickly from $\Omega_i t = 20$ to 21, with a positive effect at the contracting sides of the magnetic islands. When the two islands are merging, strong positive effect of parallel electric field acceleration can be found around $\Omega_i t = 22$. Note that after the spatial integration, the net effect of Fermi mechanism is negative during the islands merging process, which shows that the negative contributions of Fermi mechanism at the approaching sides are much stronger than the positive contributions at the contracting sides of these magnetic islands. In the second stage around $\Omega_i t = 23$, the net effect of parallel electric field mechanism is still positive, while the Fermi mechanism is still negative. In the third stage around $\Omega_i t = 24.5$, electron energization is dominated by the contribution of Fermi mechanism, while the parallel electric field contribution is very weak. From $\Omega_i t = 18$ to 30, the time evolution of the Fermi mechanism integration shows an oscillation pattern with a period about $\sim 4\Omega_i^{-1}$, which is related to the "merging-separating-merging" stages of these magnetic islands. Note that from $\Omega_i t = 18$ to 30, the time evolution of parallel electric field mechanism also shows an oscillation pattern. The results indicate an anti-phase relation between the parallel electric field mechanism (blue line) and the Fermi mechanism (red line) during the process. This is an interesting phenomenon, in which the physics under this process needs to be further studied in our future works. In these merging-separating-merging stages, the net effect of the betatron mechanism is almost negative to the electron energization, its contribution is also important to the electron acceleration and cannot be neglected in this simulation case. Figure 3(b) represents the time evolution of the spatial integration $\mathrm{d}U/\mathrm{d}t$ (corresponding to the black line, where U is the total electron kinetic energy in the simulation domain) and the sum of the contributions from the three mechanisms (corresponding to the red line). The good consistency between the black line and the red line ensures the reliability of adiabatic assumption in this simulation case with a finite guide field $B_{y0} = 0.5B_0$. Note that the small difference between $\mathrm{d}U/\mathrm{d}t$ and the "sum" comes from the non-adiabatic motion of some electrons with high thermal speed, and the motion cannot be described by a guiding-center theory.

In order to study the merging process in detail, we trace the center of the simulation domain $(0 < x < 10d_i, -0.3d_i < z < 0.3d_i)$ and integrate the contributions of the three mechanisms. The time evolution of the contributions of the three acceleration mechanisms (the average value in the range of $z = \pm 0.3d_i$) and the spatially integrated contribution from $\Omega_i t = 20$ to 30 are shown in Fig. 4. It can be found in Fig. 4(b) that the strong positive contribution of Fermi mechanism at the contracting sides and negative contribution at the approaching sides of the two magnetic islands in the first stage. The net effect of the Fermi mechanism in the first stage is positive after spatial integration, which is the dominant mechanism for electron acceleration as indicated in Fig. 4(d). Locally strong positive betatron mechanism contribution can be found in the center of these magnetic islands in the first stage, as indicated in Fig. 4(c). From $\Omega_i t = 21$ to 22 in the first stage, the contribution of parallel electric field mechanism is positive in the vicinity of the merging site, as found in Fig. 4(a). At $\Omega_i t = 22$, these two magnetic islands merge into one new island. This newly formed island expands in the x direction and is divided into two small magnetic islands in the second stage from $\Omega_i t = 22$ to 23.5, where positive contribution of the parallel electric field mechanism can be found in the vicinity of the reconnection site, as indicated in Figs. 4(a) and 4(c). The Fermi mechanism in this stage, as shown in Fig. 4(b), is positive at contracting ends of the magnetic islands while negative at two expanding ends of these islands. As the two islands are drew apart, the net effect of the Fermi mechanism is negative to electron acceleration. Figure 4(c) shows that the positive contribution of the parallel electric field mechanism and the negative contribution of the Fermi mechanism almost cancel out each other in the second stage. The sum of the three mechanisms (including the betatron mechanism) is very small for the electron acceleration in the second stage, as shown in Fig. 4(d). In the third stage where the two newly formed magnetic islands merging again from $\Omega_i t = 23.5$ to 25 , the positive contribution of the Fermi mechanism is the dominant role for the electron acceleration. However, the negative contribution of the parallel electric field mechanism is very weak due to the decrease of the reconnection rate. After the third stage, the curve of Fermi mechanism is still oscillating slightly, which may be related to the magnetic field line resonance around the boundary of the last formed magnetic island.

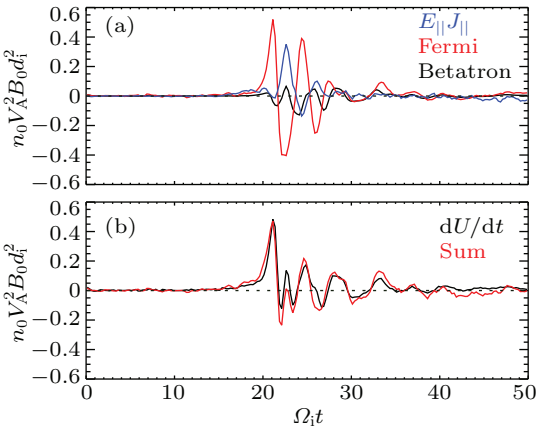


Fig. 3. (a) Time evolution of the spatially integrated contribution of the parallel electric field (blue line), Fermi (red line), and betatron (black line) mechanisms. (b) The measurement of the electron acceleration term $\mathrm{d}U/\mathrm{d}t$ and the sum of the contributions from the three mechanisms.

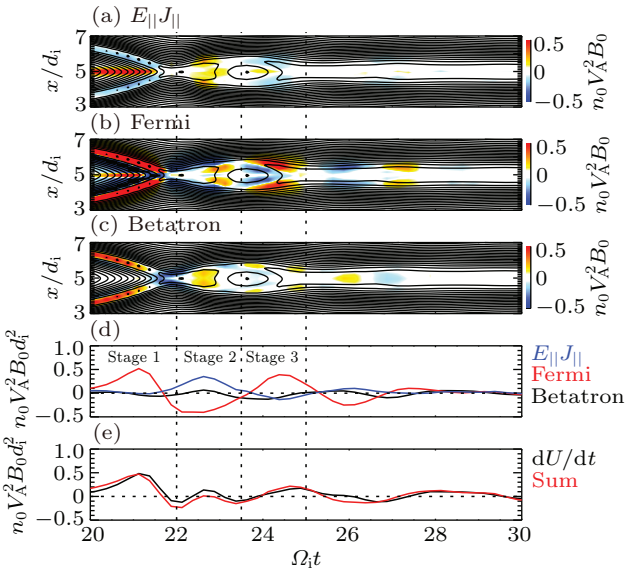


Fig. 4. (a) The temporal development of the contributions of the parallel electric field, Fermi, and betatron mechanisms (the average value in the range of $z = \pm 0.3d_i$) and (b) the spatially integrated contribution of the electron acceleration term $\mathrm{d}U/\mathrm{d}t$ and the sum of the contributions from the three mechanisms from $\Omega_i t = 20$ to 30.

4. Discussion and conclusions

In this paper, we use 2D particle-in-cell simulations with a guide field $B_{y0} = 0.5B_0$ to investigate the magnetic islands merging process. According to the time evolution of the simulation, the whole process can be divided into three stages. In the first stage, two magnetic islands approach and finally merged into a new island. Electrons can be accelerated by the Fermi mechanism at the contracting sides of the magnetic islands. However, in the vicinity of the merging site, the Fermi mechanism is negative at the approaching sides of the magnetic islands and the parallel electric field contribution is locally positive. In the second stage, the magnetic island expands in the x direction and is divided into two small magnetic islands. Parallel electric field accelerates electrons in the vicinity of the reconnection site while the contribution of the Fermi mechanism is negative at the two expanding ends of the islands. Spatial integration shows that the positive contribution of the parallel electric field mechanism and the negative contribution of the Fermi mechanism almost cancel out each other in the second stage. In the third stage, the process is similar to the first stage, in which two newly formed magnetic islands are merged into one. In this stage, electron acceleration is dominated by the Fermi mechanism while the parallel electric field is obviously weakened due to the decrease of the reconnection rate. During these three stages, both the time evolution of the spatial integrations of the Fermi mechanism and the parallel electric field mechanism showing similar oscillation patterns with a period about $\sim 4\Omega_{\mathrm{i}}^{-1}$, which is related to the merging-separating-merging stages of these magnetic islands. The time evolution of the spatial integration indicates an anti-phase relation between the parallel electric field mechanism and the Fermi mechanism during the process. This is an interesting discovery, in which the physics under this process will be further studied in our future works.

Acknowledgements

This work was supported by the National Natural Science Foundation of China (Grant Nos. 41804159 and 41774169) and the Key Research Program of Frontier Sciences, Chinese Academy of Sciences (Grant No. QYZDJ-SSW-DQC010).

References

[1] Dungey J W 1961 *Phys. Rev. Lett.* **6** 47
[2] Vasyliunas V M 1975 *Rev. Geophys. Space Phys.* **13** 303
[3] Biskamp D 2000 *Magnetic reconnection in plasmas* (Cambridge: Cambridge University Press)
[4] Birn J, Drake J F, Shay M A, Rogers B N, Denton R E, Hesse M, Kuznetsova M, Ma Z W, Bhattacharjee A, Otto A and Pritchett P L 2001 *J. Geophys. Res.* **106** 3715
[5] Lin R P and Hudson H S 1976 *Solar Phys.* **50** 153
[6] Lin R P, Krucker S, Hurford G J, Smith D M, Hudson H S, Holman G D, Schwartz R A, Dennis B R, Share G H, Murphy R J, Emslie A G, Johns-Krull C and Vilmer N 2003 *Astrophys. J. Lett.* **595** L69
[7] Miller J A, Cargill P J, Emslie A G, Holman G D, Dennis B R, LaRosa T N, Winglee R M, Benka S G, Tsuneta S 1997 *J. Geophys. Res.* **102** 14631
[8] ieroset M, Lin R P, Phan T D, Larson D E and Bale S D 2002 *Phys. Rev. Lett.* **89** 195001
[9] Imada S, Nakamura R, Daly P W, Hoshino M, Baumjohann W, Mühlbachler S, Balogh A and Rème H 2007 *J. Geophys. Res.* **112** A03202
[10] Wang R, Lu Q, Du A and Wang S 2010 *Phys. Rev. Lett.* **104** 175003
[11] Wesson J 1997 *Tokamaks* (New York: Oxford University Press)
[12] Savrukhin P V 2001 *Phys. Rev. Lett.* **86** 3036
[13] Litvinenko Y E 1996 *Astrophys. J.* **462** 997
[14] Hoshino M, Mukai T, Terasawa T and Shinohara I 2001 *J. Geophys. Res.* **106** 25979
[15] Pritchett P L 2006 *J. Geophys. Res.* **111** A10212
[16] Huang C, Lu Q and Wang S 2010 *Phys. Plasmas* **17** 072306
[17] Drake J F, Swisdak M, Che H and Shay M A 2006 *Nature* **443** 553
[18] Fu X R, Lu Q M and Wang S 2006 *Phys. Plasmas* **13** 012309
[19] Fu H, Khotyaintsev Y V, André M and Vaivads A 2011 *Geophys. Res. Lett.* **38** L16104
[20] Wu M, Lu Q, Volwerk M, Vörös Z, Zhang T, Shan L and Huang C 2013 *J. Geophys. Res.* **118** 4804
[21] Huang C, Wu M, Lu Q, Wang R and Wang S 2015 *J. Geophys. Res.* **120** 1759
[22] Wang L, Huang C, Cao X, Du A and Ge Y 2020 *J. Geophys. Res.* **125** 10
[23] Egedal J, Daughton W and Le A 2012 *Nat. Phys.* **8** 321
[24] Egedal J, Le A and Daughton W 2013 *Phys. Plasmas* **20** 061201
[25] Lu Q, Huang C, Xie J, Wang R, Wu M, Vaivads A and Wang S 2010 *J. Geophys. Res.* **115** A11208
[26] Northrop T 1963 *The Adiabatic Motion of Charged Particles* (New York: Wiley)
[27] Dahlin J T, Drake J F and Swisdak M 2014 *Phys. Plasmas* **21** 092304
[28] Numata R and Loureiro N F 2015 *J. Plasma Phys.* **81** 305810201
[29] Wang H, Lu Q, Huang C and Wang S 2016 *Astrophys. J.* **821** 84
[30] Dahlin J T, Drake J F and Swisdak M 2016 *Phys. Plasmas* **23** 120704
[31] Guo F, Li H, Daughton W and Liu Y 2014 *Phys. Rev. Lett.* **113** 155005
[32] Li X C, Guo F, Li H and Li G 2015 *Astrophys. J. Lett.* **811** L24
[33] Dahlin J T, Drake J F and Swisdak M 2015 *Phys. Plasmas* **22** 100704
[34] Muñoz P A and Büchner J 2018 *Astrophys. J.* **864** 92
[35] Pritchett P L 2008 *Phys. Plasmas* **15** 102105
[36] Chen L J, Bhattacharjee A, Puhl-Quinn P A, Yang H, Bessho N, Imada S, Mühlbachler S, Daly P W, Lefebvre B, Khotyaintsev Y, Vaivads A, Fazakerley A and Georgescu E 2008 *Nat. Phys.* **4** 19

[37] Oka M, Phan T D, Krucker S, Fujimoto M and Shinohara I 2010 *Astrophys. J.* **714** 915
[38] Wang R, Lu Q, Nakamura R, Huang C, Du A, Guo F, Teh W, Wu M, Lu S and Wang S 2015 *Nat. Phys.* **12** 263
[39] Zhao Y, Wang R, Lu Q, Du A, Yao Z and Wu M 2016 *J. Geophys. Res.* **121** 10898
[40] Wang R, Lu Q, Li X, Huang C and Wang S 2010 *J. Geophys. Res.* **115** A11201
[41] Wang R, Lu Q, Nakamura R, Baumjohann W, Russell C T, Burch J L, Ergun R E, Lindqvist P A, Wang S, Giles B and Gershman D 2017 *J. Geophys. Res.* **122** 10436
[42] Song H Q, Chen Y, Li G, Kong X L and Feng S W 2012 *Phys. Rev. X* **2** 021015
[43] Zhang T, Lu Q, Baumjohann W, Russell C, Fedorov A, Barabash S, Coates A, Du A, Cao J, Nakamura R, The W, Wang R, Dou X, Wang S, Glassmeier K, Auster H and Balikhin M 2012 *Science* **336** 567